

Energy Levels of an Ideal Quantum Ring in AA-Stacked Bilayer Graphene

Youness Zahidi^{a,b}, Abdelhadi Belouad^b and Ahmed Jellal^{*b,c}

^a*MATIC, FPK, Hassan 1 University, Khouribga, Morocco*

^b*Theoretical Physics Group, Faculty of Sciences, Chouaib Doukkali University,
PO Box 20, 24000 El Jadida, Morocco*

^c*Saudi Center for Theoretical Physics, Dhahran, Saudi Arabia*

Abstract

We theoretically analyze the energy spectrum of a quantum ring in AA-stacked bilayer graphene with radius R for a zero width subjected to a perpendicular magnetic field B . An analytical approach, using the Dirac equation, is implemented to obtain the energy spectrum by freezing out the carrier radial motion. The obtained spectrum exhibits different symmetries and for a fixed total angular momentum m , it has a hyperbolic dependence of the magnetic field. In particular, the energy spectra are not invariant under the transformation $B \rightarrow -B$. The application of a potential, on the upper and lower layer, allows to open a gap in the energy spectrum and the application of a non zero magnetic field breaks all symmetries. We also analyze the basics features of the energy spectrum to show the main similarities and differences with respect to ideal quantum ring in monolayer, AB-stacked bilayer graphene and a quantum ring with finite width in AB-stacked bilayer graphene.

PACS numbers: 81.05.ue, 81.07.Ta, 73.22.Pr.

Keywords: Ideal quantum ring, AA-bilayer graphene, magnetic field, energy spectrum.

*ajellal@ictp.it – jellal.a@ucd.ac.ma

1 Introduction

Graphene, an isolated single layer of graphite, since its isolation in 2004 [1] has attracted many experimental and theoretical research activities. This led to discovery of many interesting properties [2] not been observed in the ordinary two dimensional electron gas. The large interest is due to both the unusual mechanical and electronic properties as well as for the prospects of applications, which may lead to their use in novel nanoelectronic devices. In addition, graphene offers the remarkable possibility to probe predictions of quantum field theory in condensed matter systems, as its low-energy spectrum is described by the Dirac-Weyl Hamiltonian of massless fermions [3]. These different properties of graphene are related to the unusual electronic structure of graphene, in which the charge carriers behave as massless fermions with a gapless linear dispersion.

Graphene can not only exist in the free state, but two or more layers can stack above each other to form what is called few layer graphene. As example for two coupled graphene sheets, it is known as bilayer graphene. Bilayer graphene systems show interesting properties with strong dependence on stacking. In bilayer graphene there are four atoms per unit cell, with inequivalent sites A_1 , B_1 and A_2 , B_2 in the first and second graphene layers, respectively. There are two dominant ways in which the two layers can be stacked. The first one is the so called AB-stacked bilayer graphene [4,5] and the second is the AA-stacked bilayer graphene [6,7]. In the AB-stacking, the layers are arranged in such a way that the A_1 sublattice is exactly on top of the sublattice B_2 . In the AA-stacking, both sublattices of one sheet A_1 and B_1 , are located directly on top of the two sublattices of the other sheet A_2 and B_2 .

Recently, bilayer graphene has surged as another attractive two-dimensional carbon material and demonstrated new unusual physical properties [8–14]. In fact, bilayer graphene is a very different material from monolayer graphene and also from graphite. The AB-stacked bilayer graphene has a gapless quadratic dispersion relation, two conduction bands and two valance bands, each pair is separated by an interlayer coupling energy of order $\gamma_1 = 400\text{meV}$. However, the energy bands for AA-stacked bilayer graphene are just the double copies of single layer graphene bands shifted up and down by the interlayer coupling $\gamma = 200\text{meV}$. By applying a perpendicular electric field on the upper and lower layer, the spectrum is found to display a gap, which can be tuned by varying the bias or by chemical doping of the surface [15]. This tunable gap can then be exploited for the development of bilayer graphene devices. In particular, the possibility of controlling the energy gap has raised the possibility of the creation of electrostatically defined quantum dots [16,17] and quantum ring [18,19] in bilayer graphene.

Quantum rings in graphene have also attracted some interest. They are expected to find application in microelectronics as well as in future quantum information devices. In fact, a very important class of quantum devices consists of quantum rings. It have been studied in semiconductor systems, both experimentally and theoretically [20]. Recently, quantum rings have been studied both theoretically and experimentally in monolayer graphene [21,22]. The graphene-based quantum rings have been obtained experimentally by lithographic techniques [22]. These systems have been studied theoretically in monolayer graphene. Two different ring systems are considered: a ring with a smooth boundary and a hexagonal ring with zigzag edges [23]. For AB-stacked bilayer graphene, it was shown that it is possible to electrostatically confine quantum ring with a finite width [18].

In this work, we consider a quantum ring in AA-stacked bilayer graphene in the presence of an external magnetic field. We obtain analytical expression of the energy spectrum by solving the Dirac equation and freezing out the carrier radial motion, for zero and non zero magnetic field. The obtained energy spectrum for ideal quantum ring will be investigated numerically to underline the behavior of our system. We investigate the basic features of our results and compare them with those for ideal ring in monolayer graphene and AB-stacked bilayer graphene and also for quantum ring with finite width in AB-stacked bilayer graphene.

The set of the paper is organized as follows. In section 2, we present our problem by setting the Hamiltonian describing the system under consideration. Subsequently, we use the eigenvalue equation to find the analytic expressions for the energy spectrum. In section 3, we present our results and give different discussions. Section 4 provides a summary and conclusions.

2 Problem setting

We consider an AA-stacked bilayer graphene quantum ring. This system is characterized by two monolayer sheets stacked directly on top of each other. Each carbon atom of the upper layer is located above the corresponding atom of the lower layer and they are separated by an interlayer coupling energy γ (see Figure 1).

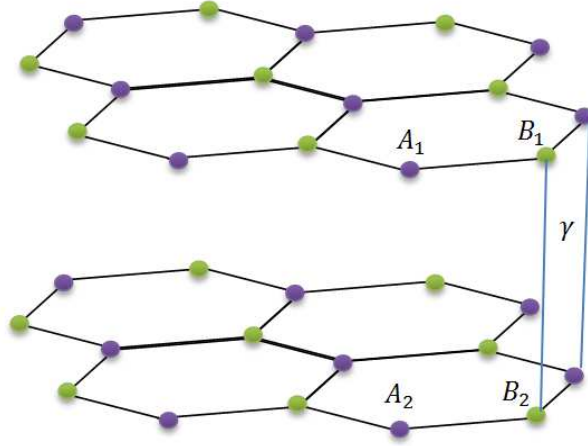


Figure 1: Schematic illustration of lattice structure of AA-stacked bilayer graphene. It is composed of two graphene layers.

The Hamiltonian in the vicinity of the K and K' valleys, of the first Brillouin zone, with a perpendicular magnetic field, can be written as

$$\mathcal{H} = \begin{pmatrix} \tau U & \boldsymbol{\pi} & \gamma & 0 \\ \boldsymbol{\pi}^\dagger & \tau U & 0 & \gamma \\ \gamma & 0 & -\tau U & \boldsymbol{\pi} \\ 0 & \gamma & \boldsymbol{\pi}^\dagger & -\tau U \end{pmatrix}. \quad (1)$$

Here $\gamma = 200\text{meV}$ is the interlayer coupling term [24], $\boldsymbol{\pi} = v_F(\mathbf{p} + e\mathbf{A})$ with \mathbf{p} being the two-dimensional momentum operator, in which the symmetric gauge is used to describe the vector potential

\mathbf{A} , $v_F = 10^6$ m/s is the Fermi velocity and $\tau = \pm 1$ distinguishes the two K and K' valleys. Moreover, the application of a perpendicular electric field creates a potential $+U$ in the upper layer and $-U$ in the lower layer [25–27]. For the AA-stacked bilayer graphene, the Hamiltonian (1) acts on a four component spinor $[\Psi_{A_1}, \Psi_{B_1}, \Psi_{A_2}, \Psi_{B_2}]^T$, where $\Psi_{A_1(A_2)}$ and $\Psi_{B_1(B_2)}$ are the envelope functions associated with the probability amplitudes of the wave functions on the $A_1(A_2)$ and $B_1(B_2)$ sublattices of the upper (lower) layer. Since the total angular momentum operator J_z commutes with \mathcal{H} , then we can construct a common basis in terms of the eigenspinors, in the polar coordinates such as $\Psi(r, \theta) = e^{im\theta} [\Phi_{A_1}(r)e^{i\theta}, i\Phi_{B_1}(r), \Phi_{A_2}(r)e^{i\theta}, i\Phi_{B_2}(r)]^T$, where m is the angular momentum label. Using the symmetric gauge $\mathbf{A} = (0, \frac{Br}{2}, 0)$, to write the corresponding momentum operators as

$$\boldsymbol{\pi} = v_F e^{i\theta} \left[-i\hbar \left(\frac{\partial}{\partial r} + \frac{i\partial}{r\partial\theta} \right) + i \frac{eBr}{2} \right] \quad (2)$$

$$\boldsymbol{\pi}^\dagger = v_F e^{-i\theta} \left[-i\hbar \left(\frac{\partial}{\partial r} - \frac{i\partial}{r\partial\theta} \right) - i \frac{eBr}{2} \right]. \quad (3)$$

In the next we will present analytical expression of the eigenstates and energy levels of ideal quantum ring created with AA-stacked bilayer graphene. For an ideal ring with radius R , the momentum of the charge carriers in the radial direction is zero. By freezing out the carrier radial motion, the four-component wave function becomes

$$\Psi(R, \theta) = \begin{pmatrix} \Phi_{A_1}(R)e^{i\theta} \\ i\Phi_{B_1}(R) \\ \Phi_{A_2}(R)e^{i\theta} \\ i\Phi_{B_2}(R) \end{pmatrix} e^{im\theta}. \quad (4)$$

By solving the Dirac equation $\mathcal{H}\Psi(R, \theta) = E\Psi(R, \theta)$, we obtain the following system of coupled differential equations

$$\begin{cases} (E - \tau U)\Phi_{A_1}(R) - \eta(m + \beta)\Phi_{B_1}(R) + \gamma\Phi_{A_2}(R) & = 0 \\ \eta(m + \beta + 1)\Phi_{A_1}(R) - (E + \tau U)\Phi_{B_1}(R) - \gamma\Phi_{B_2}(R) & = 0 \\ \eta(m + \beta + 1)\Phi_{A_2}(R) - (E - \tau U)\Phi_{B_2}(R) - \gamma\Phi_{B_1}(R) & = 0 \\ \gamma\Phi_{A_1}(R) - \eta(m + \beta)\Phi_{B_2}(R) + (E + \tau U)\Phi_{A_2}(R) & = 0 \end{cases} \quad (5)$$

where we have set the quantities

$$\eta = \frac{\hbar v_F}{R}, \quad \beta = \frac{eB}{2\hbar} R^2. \quad (6)$$

After some straightforward algebra, we end up with the polynomial equation that determine the energy spectrum

$$E^4 - 2E^2(\eta^2\alpha + U^2 + \gamma^2) + (\eta^2\alpha + U^2)^2 - 2(\eta^2\alpha - U^2)\gamma^2 + \gamma^4 = 0 \quad (7)$$

where the parameter α is given by

$$\alpha = (m + \beta)^2 + (m + \beta). \quad (8)$$

There are four solutions for (7)

$$E = s\sqrt{(\gamma \pm \eta\sqrt{\alpha})^2 + U^2} \quad (9)$$

with $s = \text{sign}(E)$. We notice that for $m + \beta \leq -1$ or $m + \beta \geq 0$ the four solutions are real, except for $-1 < m + \beta < 0$, which they are complex.

3 Results and discussions

In Figure 2, we plot the energy levels of an ideal quantum ring in AA-stacked bilayer graphene as a function of the ring radius R with $-10 \leq m \leq 10$. The green and red curves correspond, respectively, to $-10 \leq m \leq -1$ and $1 \leq m \leq 10$, while the blue one corresponds to $m = 0$. For $U = 0\text{meV}$ (Figure 2(a) and (c)), we see that the energy spectrum shows two set of levels and the energy spectrum for $U = 0\text{meV}$ resembles those found in the case of AA-stacked bilayer graphene quantum dot [28]. It is clear that the two set of this AA-stacked bilayer are just double copies of the energy spectrum corresponding to monolayer graphene one, shifted up/down by $= +/ - \gamma$. We notice that for zero magnetic field, the energy take the following form

$$E(m, \beta = 0) = s\sqrt{(\gamma \pm \eta\sqrt{m(m+1)})^2 + U^2}. \quad (10)$$

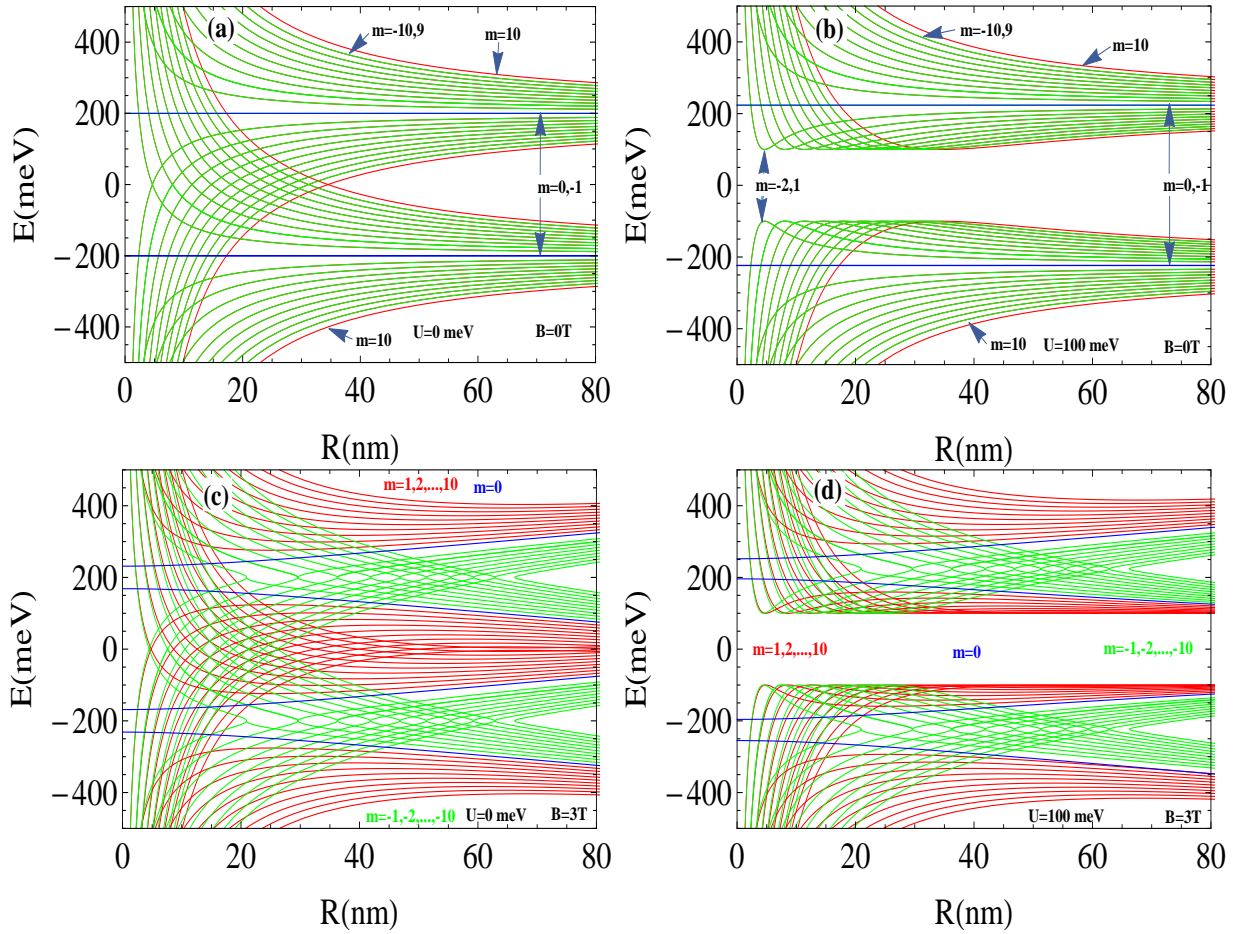


Figure 2: Energy as function of the radius R for an ideal quantum ring in AA-stacked bilayer graphene with the angular quantum number $-10 \leq m \leq -1$ (green curves), $1 \leq m \leq 10$ (red curves) and $m = 0$ (blue curves). (a): Zero magnetic field $B = 0\text{T}$ and $U = 0\text{meV}$. (b): Zero magnetic field $B = 0\text{T}$ and $U = 100\text{meV}$. (c): Non zero magnetic field $B = 3\text{T}$ and $U = 0\text{meV}$. (d): Non zero magnetic field $B = 3\text{T}$ and $U = 100\text{meV}$.

It is important to note that for $\gamma = 0$, we recover the energy of monolayer graphene [19]. For large ring radius R , the upper set of levels converges to the interlayer hopping energy $\gamma = 200\text{meV}$. However, the

lower set of levels converges to $\gamma = -200\text{meV}$. In addition, we notice that from (10) and for $m = 0, -1$ the energy will be independent of the radius R

$$E = s\sqrt{\gamma^2 + U^2} \quad (11)$$

and therefore all branches are twofold degenerate. Furthermore, (10) exhibits interesting spectrum symmetries, such as

$$E(m, 0) = E(-m - 1, 0) \quad (12)$$

$$E(0, 0) = E(-1, 0). \quad (13)$$

The application of a potential, on the upper and lower layer, allows to open a gap in the energy spectrum (Figure 2(b) and (d)). When the ring radius increases, for zero magnetic field, the gap width increases as well, which can be seen clearly in Figure 2(b). Note that, in the case of a quantum ring with finite width [18], the results show a weak dependence on the ring radius.

Furthermore, the numerical results demonstrate that the application of a non zero magnetic field ($B = 3\text{T}$) break the degeneracy of all branches. In contrast with the results obtained from the Schrödinger equation, the electron and hole energy levels are not invariant under the transformation $B \rightarrow -B$ [18]. These results are similar to those obtained for an ideal quantum ring in monolayer and AB-stacked bilayer graphene [19] and also for quantum ring with finite width [18]. For non zero magnetic field and for large ring radius R , (10) becomes

$$E(m, \beta) = s\sqrt{(\gamma \pm \lambda R)^2 + U^2} \quad (14)$$

where the parameter $\lambda = \frac{eBv_F}{2}$ is magnetic field dependent. This can clearly explain the approximately linear dependence of the energy branches on the ring radius for large R . However, for small R , (14) reduces to the form

$$E(m, \beta) = s\frac{\hbar v_F}{R}\sqrt{m(m+1)} \quad (15)$$

showing that the spectrum has $1/R$ dependence. In addition, like the case of zero magnetic field, the application of a potential open a gap in the energy spectrum. But, the gap width remains unchanged by increasing ring radius R .

In Figure 3, we plot the energy levels of an ideal quantum ring as function of the angular momentum m for three different values of the magnetic field ($B = -3\text{T}, 0\text{T}, 3\text{T}$), with $U = 100\text{meV}$ and $R = 50\text{nm}$. We notice that, like the case of monolayer [19] and AB-stacked bilayer graphene [29], the electron energy presents a minimum for a particular value of the angular momentum m . The minimum energy for $B = -3\text{T}$ is given by two values of m : $m = 20$ and $m = -10$. However, the minimum energy for $B = 0\text{T}$ and $B = 3\text{T}$, are respectively, given by $m = 15, -16$ and $m = 9, -21$. This can be explained by the fact that from (9), the spectra are invariant under the transformation $B \rightarrow -B$ and $m \rightarrow -(m+1)$. Thus, the energies are related by the symmetry relation

$$E(m, B) = E(-m - 1, -B) \quad (16)$$

which is also exists in the case of an ideal quantum ring in monolayer graphene [19].

The magnetic field dependence of the energy spectrum is presented in Figure 4 with the ring radius $R = 50\text{nm}$ and $U = 0\text{meV}$ (Figure 4(a)) and $U = 100\text{meV}$ (Figure 4(b)). The green and red curves,

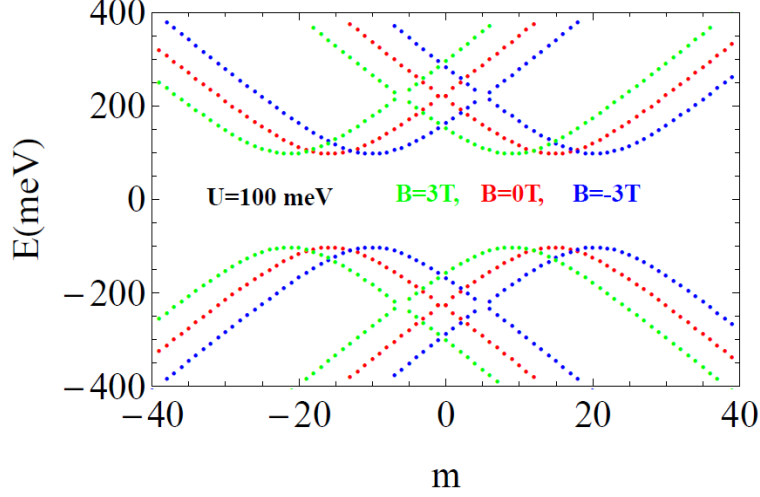


Figure 3: Energy levels of an ideal quantum ring in AA-stacked bilayer graphene as function of the angular momentum m for $B = -3T, 0T, 3T$, with $U = 100\text{meV}$ and $R = 50\text{nm}$.

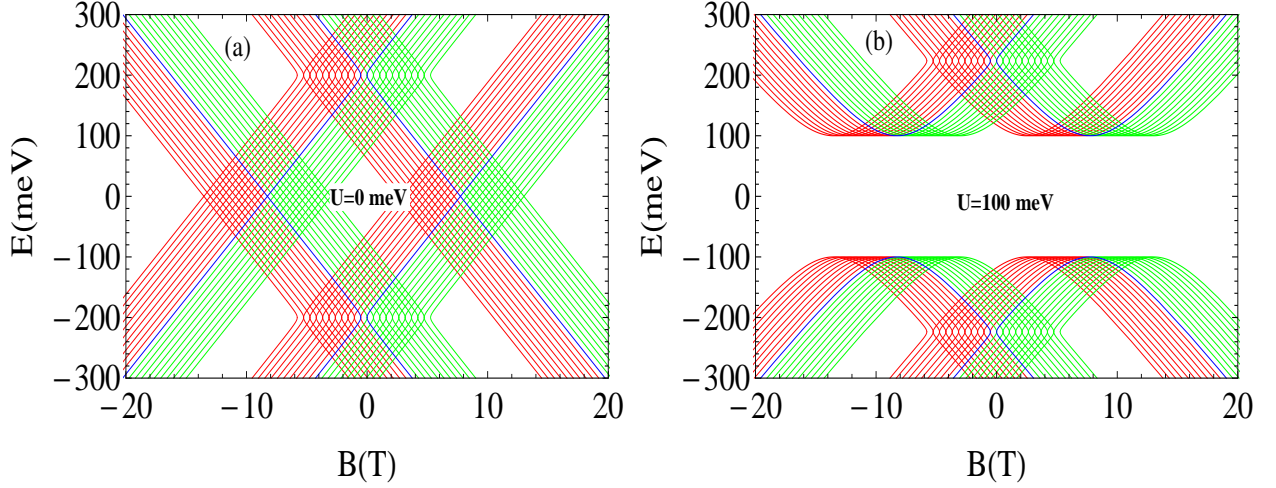


Figure 4: Energy spectrum of an ideal quantum ring in AA-stacked bilayer graphene as function of the magnetic field B for $R = 50\text{nm}$ with (a): $U = 0\text{meV}$ and (b): $U = 100\text{meV}$. The energy levels are shown for the quantum number $-10 \leq m \leq -1$ (green curves), $1 \leq m \leq 10$ (red curves) and $m = 0$ (blue curves).

respectively, show the energy for $-10 \leq m \leq -1$ and $1 \leq m \leq 10$. However, the blue curves show the energy for $m = 0$. In Figure 4(a), we plot the electron and hole energy levels for ideal quantum ring in AA-stacked bilayer graphene for $U = 0\text{meV}$, where (9) reduces to

$$E = s(\gamma \pm \eta\sqrt{\alpha}). \quad (17)$$

We can clearly show that the energy levels are straight lines and we have zero gap. Moreover, one can see that the energy spectrum shows two set of levels. They are just the double copies of the energy spectrum corresponding to ideal quantum ring in monolayer graphene, one shifted up by $+\gamma$ and other one shifted down by $-\gamma$, where $\gamma = 200\text{meV}$. We notice that the energy spectrum resembles those found in the case of monolayer graphene for ideal quantum ring [19] and for hexagonal ring with

zigzag edges [23]. In Figure 4(b), the energy has a hyperbolic dependence of the magnetic field. In addition, the application of a potential $U = 100\text{meV}$ leads to the appearance of a energy gap around the point $E = 0$. Also, these results show that the electron energy spectrum exhibits a minimum at $E = U$ and there is a symmetry between the electron and hole states. Indeed, the electron and hole energies are related by the symmetry

$$E_e(m, B) = -E_h(-m - 1, -B) \quad (18)$$

where the indices h and e refer, respectively to holes and electrons. These results are not similar to that obtained for a finite width quantum ring in AB-stacked bilayer graphene [19], where the electron energy exhibits two local minima and the electron and hole states are asymmetric.

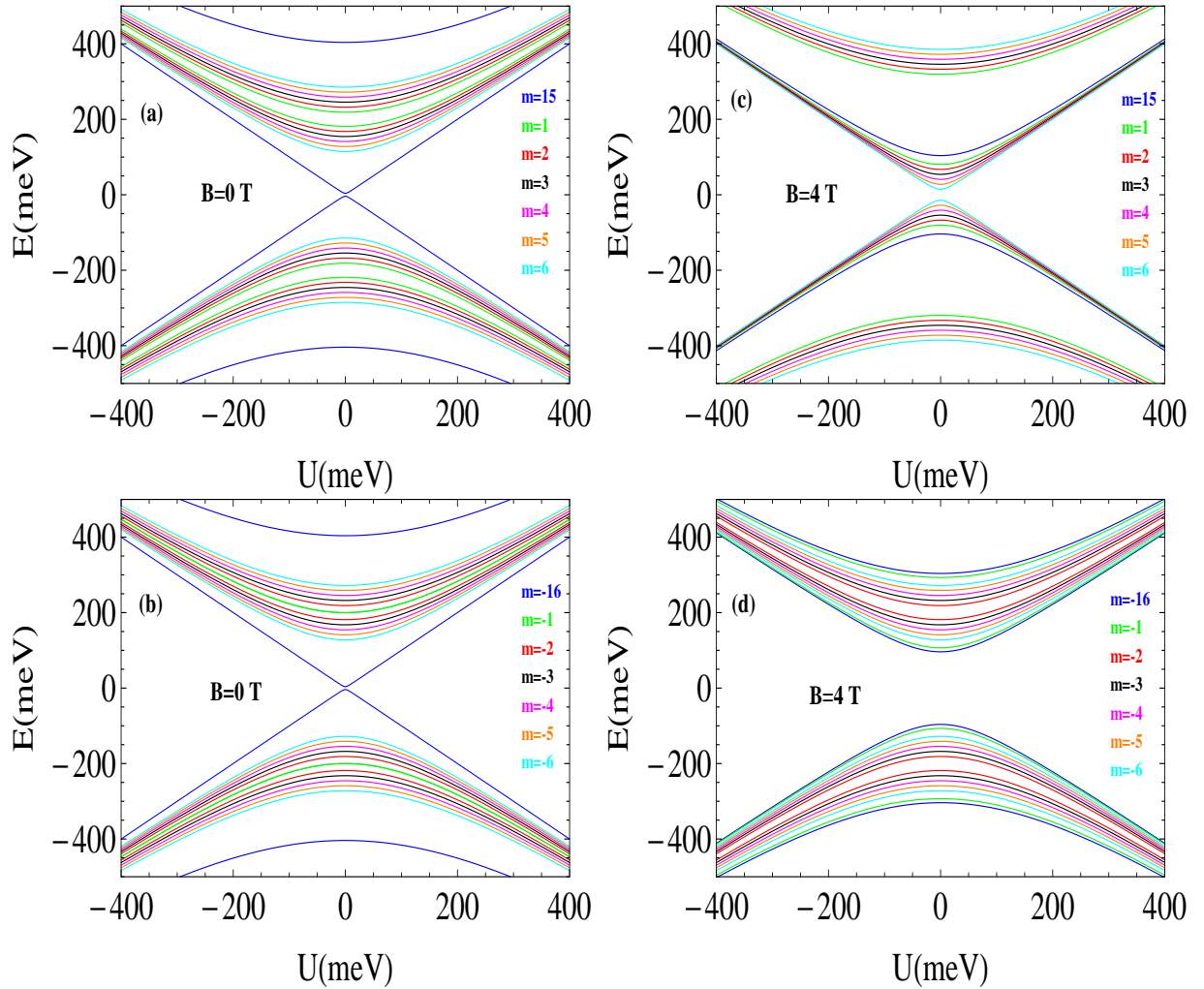


Figure 5: Energy levels of an ideal quantum ring in AA-stacked bilayer graphene as function of the potential U with $R = 50\text{nm}$. (a): $B = 0\text{T}$ and $m > 0$. (b): $B = 0\text{T}$ and $m < 0$. (c): $B = 4\text{T}$ and $m > 0$. (d): $B = 4\text{T}$ and $m < 0$.

In Figure 5, we plot the energy spectrum as a function of the potential U with $R = 50\text{nm}$, for zero magnetic field (left panels) and $B = 4\text{T}$ (right panels) with positive m (upper panels) and negative m (lower panels). For zero magnetic field the energy spectrum has an hyperbolic form and is twofold

degenerate due to the fact that we have $E(m) = E(-m - 1)$. Note that an energy gap is opened for non zero magnetic field. These results are similar to the case of a quantum ring in monolayer graphene where the energy gap is opened by applying a non zero magnetic field [19]. In the case of AB-stacked bilayer graphene, the results are similar to those found for a quantum ring in monolayer graphene where the gate potential has a similar effect as the mass term. The application of a non zero magnetic field break the degeneracy.

4 Conclusion

In summary, we have investigated a quantum ring in AA-stacked bilayer graphene by including the effect of an external magnetic field. The calculation was performed by solving the Dirac equation for a zero width ring geometry, i.e. ideal ring. In the case of an ideal ring with radius R , the momentum of the carriers in the radial direction is zero, then we have treat the radial parts of the spinors as a constant. From the eigenvalue equation, we have obtained the energy spectrum as function of the ring radius, the potential and the magnetic field.

Our numerical results showed that the energy spectrum of ideal quantum ring presents two sets of states as function of the ring radius R . The upper set corresponds to the upper layer and the lower one corresponds to the lower layer. By increasing the ring radius, for zero magnetic field, the upper set of levels converges to the interlayer hopping energy $\gamma = 200\text{meV}$ and the lower set levels converges to $\gamma = -200\text{meV}$. In the absence of the magnetic field, the energy levels are twofold degenerate where $E(m, 0) = E(-m - 1, 0)$. It is important to note that the application of a potential, on the upper and lower layer, allows to open a gap in the energy spectrum. By increasing the ring radius R , the gap width increases as well. These results differs from previous studies of graphene-based quantum ring with finite width, where the energy levels show a weak dependence on the ring radius.

Furthermore, our numerical results demonstrated that the electron and hole energy levels are not invariant under the transformation $B \rightarrow -B$. These results are similar to that obtained for ideal ring in monolayer and AB-stacked bilayer graphene and also for a quantum ring with finite width in AB-stacked bilayer graphene. However, it is not the case with the results obtained from the Schrödinger equation. We notice that the application of a non zero magnetic field breaks the degeneracy of all branches. For small ring radius, the energy branches have a $1/R$ dependence. For large ring radius, the branches have an approximately linear dependence on the ring radius. We have found also that the field dependence is linear for a fixed total angular momentum m for $U = 0\text{meV}$. However, for $U = 100\text{meV}$, the energy has a hyperbolic dependence of the magnetic field and exhibits a minimum for a special values of m . In addition, the application of a potential $U = 100\text{meV}$ leads to the appearance of a energy gap around $E = 0$.

Acknowledgment

The generous support provided by the Saudi Center for Theoretical Physics (SCTP) is highly appreciated by all authors.

References

- [1] K. S. Novoselov, A. K. Geim, S. M. Morozov, D. Jiang, Y. Zhang, S. V. Dubonos, I. V. Grigorieva and A. A. Firosov, *Science* 306, 666 (2004).
- [2] A. H. Castro Neto, F. Guinea, N. M. R. Peres, K. S. Novoselov and A. K. Geim, *Rev. Mod. Phys.* 81, 109 (2009).
- [3] A. K. Geim and K. S. Novoselov, *Nat. Mater.* 6, 183 (2007).
- [4] J. D. Bernal, *Phys. Eng. Sci.* 106, 749 (1924).
- [5] J. C. Charlier, J. P. Gonze and X. Michenaud, *Phys. Rev. B* 43, 6 (1991).
- [6] J.-K. Lee, S.-C. Lee, J.-P. Ahn, S.-C. Kim, J. I. B Wilson and P. John, *J. Chem. Phys.* 129, 234709 (2008).
- [7] P. L. de Andres, R. Ramirez and J. A. Vergs, *Phys. Rev. B* 77, 045403 (2008).
- [8] E. McCann, *Phys. Rev. B* 74, 161403 (2006).
- [9] T. Ohta, A. Bostwick, T. Seyller, K. Horn and E. Rotenberg, *Science* 313, 951 (2006).
- [10] J. M. Pereira, Jr., F. M. Peeters and P. Vasilopoulos, *Phys. Rev. B* 76, 115419 (2007).
- [11] S. Y. Zhou, G.-H. Gweon, A. V. Fedorov, P. N. First, W. A. de Heer, D.-H. Lee, F. Guinea, A. H. Castro Neto and A. Lanzara, *Nature Mater.* 6, 770 (2007).
- [12] J. B. Oostinga, H. B. Heersche, X. Liu, A. F. Morpurgo and L. M. K. Vandersypen, *Nature Mater.* 7, 151 (2008).
- [13] Y. Zhang, T. T. Tang, C. Girit, Z. Hao, M. C. Martin, A. Zettl, M. F. Crommie, Y. R. Shen and F. Wang, *Nature* 459, 820 (2009).
- [14] S. B. Kumar and J. Guo, *Appl. Phys. Lett.* 98, 222101 (2011).
- [15] E. McCann and V. I. Fal'ko, *Phys. Rev. Lett.* 96, 086805 (2006).
- [16] J. M. Pereira, Jr., P. Vasilopoulos and F. M. Peeters, *Nano Lett.* 7, 946 (2007).
- [17] J. M. Pereira, Jr., P. Vasilopoulos, F. M. Peeters and G. A. Farias, *Phys. Rev. B* 79, 195403 (2009).
- [18] M. Zarenia, J. M. Pereira, Jr., F. M. Peeters and G. A. Farias, *Nano Lett.* 9, 4088 (2009).
- [19] M. Zarenia, J. M. Pereira, A. Chaves, F. M. Peeters and G. A. Farias, *Phys. Rev. B* 81, 045431 (2010).
- [20] A. Fuhrer, S. Lscher, T. Ihn, T. Heinzel, K. Ensslin, W. Wegscheider and M. Bichler, *Nature (London)* 413, 822 (2001).

- [21] S. Russo, J. B. Oostinga, D. Wehenkel, H. B. Heersche, S. S. Sobhani, L. M. K. Vandersypen and A. F. Morpurgo, Phys. Rev. B 77, 085413 (2008).
- [22] M. Huefner, F. Molitor, A. Jacobsen, A. Pioda, C. Stampfer, K. Ensslin and T. Ihn, New J. Phys. 12, 043054 (2010).
- [23] P. Recher, B. Trauzettel, A. Rycerz, Ya. M. Blanter, C. W. J. Beenakker and A. F. Morpurgo, Phys. Rev. B 76, 235404 (2007).
- [24] C. J. Tabert and E. J. Nicol, Phys. Rev. B 86, 075439 (2012).
- [25] D. Wang, Phys. Lett. A 375, 4070 (2011).
- [26] D. Wang and G. Jin, J. Appl. Phys. 112, 053714 (2012)
- [27] D. Wang and G. Jin, Phys. Lett. A 377, 2901 (2013).
- [28] A. Belouad, Y. Zahidi and A. Jellal, Mater. Res. Express 3, 055005 (2016).
- [29] D. R. da Costa, M. Zarenia, A. Chaves, G. A. Farias and F. M. Peeters, Carbon 78, 392 (2014).